

THE WELDED JOINTS STRUCTURE OF THE INCONEL 617 ALLOY DESIGNED FOR HIGH TEMPERATURE OPERATION IN SUPERCRITICAL PARAMETERS BOILERS

The development of power industry obligates designers, materials engineers to create and implement new, advanced materials, in which Inconel 617 alloy is included. Nowadays, there are a lot of projects which describe microstructure and properties of Inconel 617 alloy. However, the welded joints from mentioned material is not yet fully discussed in the literature. The description of welded joints microstructure is a main knowledge source for designers, constructors and welding engineers in estimating durability process and degradation assessment for elements and devices with welds of Inconel 617 alloy. This paper presents the analysis and assessment of advanced nickel alloy welded joints, which have been done by tungsten inert gas (TIG). Investigations have included analysis made by light microscope and scanning electron microscope. The disclosed precipitates were identified with Energy Dispersive Spectroscopy (EDS) microanalysis, then it were done X-Ray Diffraction (XRD) phases analysis. To confirm the obtained results, a scanning-transmission electron microscope (STEM) analysis was also performed.

The purpose of the article was to create a comprehensive procedure for revealing the Inconel 617 alloy structure. The methodology presented in this article will be in future a great help for constructors, material specialists and welding engineers in assessing the structure and durability of the Inconel 617 alloy.

Keywords: Inconel 617; nickel alloys; welded joint; macrostructure; microstructure; etching; TIG method

1. Introduction

The global power industry is constantly developing. This stems from a high demand for electricity, the limited availability of fossil fuels, as well as restrictions related to the increasing environmental pollution. The main direction for the development of the power industry include increased security of fuel and energy supply, enhanced energy efficiency, as well as the development of the nuclear energy and renewable energy sectors, leading to a decreased impact of the power industry on the environment [1-3]. This development requires the use of new energy processing technologies and new materials working in complex conditions.

The design of high-pressure components for new power units is a challenge for structural engineers and material engineers. Since the 1980s, research programmes aimed at introducing new structural materials onto the energy market have been carried out. One of the groups of materials that show the greatest potential for application in the modern power industry are nickel-based alloys. In recent years, these alloys have undergone major

development, both in terms of the manufacturing technologies and in terms of their properties [1,4-5].

Nickel-based alloys are characterised by good physico-chemical and mechanical properties at high temperatures, including creep resistance, high-temperature corrosion resistance, thermo-mechanical fatigue resistance, and structural stability. A material that can be used for a very wide range of supercritical and ultra-supercritical boiler components is Inconel 617, which is particularly useful under creep conditions at high temperatures and under high-temperature corrosion conditions [6,7].

According to the literature [8,9], the TIG method is one of the best joining method of advanced nickel alloys and it should be used to connect Inconel 617 alloy because of the high quality of welded joints. As an additional welding material, it is need to use material with similar chemical composition. For welding nickel alloy of Inconel 617 was used ERNiCrCoMo-1 welding wire with diameter of 2,4 mm. While welding mentioned advanced alloy, it is need to use as low heat input as possible to prevent welding incompatibilities, e.g. crackings [8-11].

¹ SILESIAAN UNIVERSITY OF TECHNOLOGY FACULTY OF MATERIALS ENGINEERING AND METALLURGY, INSTITUTE OF MATERIALS ENGINEERING, 8 KRASIŃSKIEGO STR., 40-019 KATOWICE, POLAND

* Corresponding author: natalia.konieczna@polsl.pl



If the service properties of the alloy and its welded joints are to be assessed correctly, the structure of the alloy needs to be precisely described. This is particularly important in the case of welded joints involving major structural heterogeneity resulting from the welding process. The literature provides no clear information on the methodology for assessing the structure of such alloys. Thus, it is necessary to systematize such assessment and establish a clear procedure for describing the structure of Inconel 617, which is the main objective of this paper.

2. Test material

The samples were 1, 3, and 5 mm thick plates of Inconel 617 (UNS N06617 according to ASME SB-168:2013), manufactured by TyssenKrupp VDM. The chemical composition (Table 1) was verified by X-ray fluorescence (XRF). The tests were carried out using a Niton XL2 spectrometer. An example of an XRF spectrum is shown in Fig. 1.

The results of the measurement of the percentage of elements in Inconel 617 showed that the material met the requirements of ASME SB-168:2013 and that the element contents indicated in the specifications fell within the acceptable limits set out in that standard. Moreover, small amounts of niobium were found in the material (below 0.2%). Niobium is a strong carbide former; it forms fine-sized, compound, strengthening carbonitrides [12,13].

3. Procedure for describing the structure of Inconel 617

In order to assess the macro- and microstructure of Inconel 617, it is necessary to develop a methodology including a quality-oriented procedure that ensures legible and repeatable results and at the same time requires reasonable effort. A qualitative description of the structure is necessary to identify clear correlations in the following cause and effect chain: chemical composition → manufacture technology → structure → service properties.

3.1. Selection of the sampling area for structural examinations

The manner of sampling and the number of samples depend on the repeatability of chemical composition and structure within the same component and within an entire batch. This is particularly important for welded joints that are very heterogeneous both in terms of the chemical composition and in terms of the structure. This stems from changes in parameters affects during welding and from the mixing of the material in the weld pool. This changeability the manner of sampling and the number of areas analysed for each sample. Thus, the homogeneity of the chemical composition, the size and shape of the welded joint, and the welding procedure employed are major factors affecting the sampling strategy.

TABLE 1

The chemical composition of Inconel 617 alloy according to ASME SB-168:2013 standard

Ni	Cr	Co	Mo	Al	Fe	Mn	Si	Ti	Cu	S	B	C
min. 44.5	20.0÷24.0	10.0÷15.0	8.0÷10.0	0.80÷1.50	max. 3.0	max. 1.0	max. 1.0	max. 0.6	max. 0.5	max. 0.015	max. 0.006	0.05÷0.15

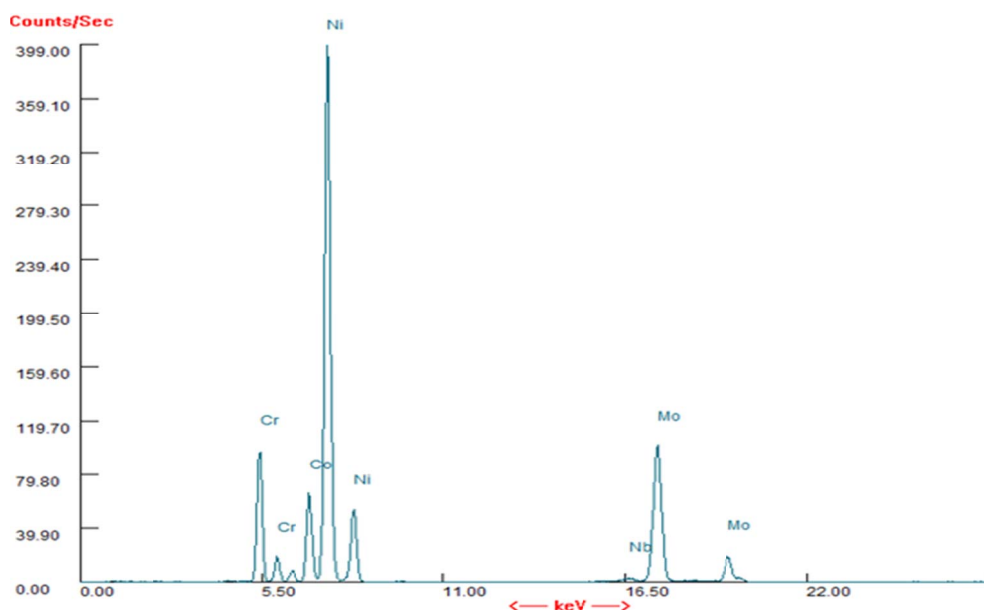


Fig. 1. An example of an XRF spectrum for Inconel 617, plate thickness: 3 mm

In the case of welded joints, samples for structural examinations should be collected perpendicularly to the welding direction (Fig. 2). This ensures that all areas typical of a welded joint will be analysed, i.e. the base material, the heat affected zone, and the weld. When collecting samples, special attention should be paid to the possibility that the area concerned will become overheated as a result of the cutting process. If this is the case, samples should be taken from an area located at least 20 mm away from the overheated area along the welding direction.

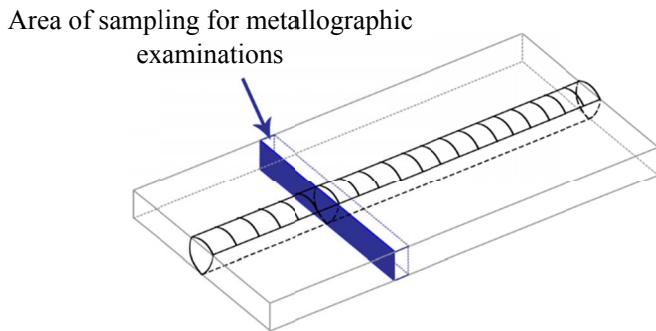


Fig. 2. Diagram showing the sample cutting area for metallographic examinations of Inconel 617 welded joints

3.2. Method for preparing metallographic sections

A methodology for preparing metallographic sections should guarantee that a mirror-like surface without artifacts is obtained, with the cutting, grinding, and polishing taking a reasonable amount of time.

The procedure proposed herein assumes that the cutting process comprises two stages. The rough cutting of the Inconel 617 samples was carried out using a Buehler Delta Abrasimet Cutter; at the second stage, a Buehler Isomet 5000 was used for precision cutting. The cutting parameters are shown in Table 2.

The cut-out samples, due to their shape, were appropriately mounted for the purposes of the next stages of the procedure, i.e. grinding and polishing. Thermosetting phenolic resins with a

TABLE 2

Inconel 617 cutting parameters for the rough and precision cutters

Device name	Cooling medium	Blade type and measurements	Rotation speed, rpm	Cutting rate, mm/min
Delta Abrasimer	Coolmet	Buehler 95-B2211-010 250 × 1.5 × 32	4000	10÷15
Isomet 5000	Coolmet	Buehler 95-B2211-010 178 × 0.76 × 12.7	4000	1.2÷1.5

conductive filler were used for the mounting [14,15]. A conductive filler enables sample observation under a scanning electron microscope (SEM).

Such prepared metallographic sections were ground manually using 120-1200 grit abrasive papers (Table 2, items 1-5). The surface quality was inspected using a light microscope at 100× magnification. After sections with no artifacts were obtained, the next stage was polishing with diamond paste. The polishing parameters are presented in Table 2, items 6 and 7. It was concluded that the proposed procedure for preparing metallographic sections of Inconel 617 welded joints ensures that a mirror-like surface without artifacts is obtained within approx. 10 min.

3.3. Selecting the reagent for chemical etching

The selection of a reagent for etching metallographic sections is an important factor in the revealing of the structure and thus it determines the quality of the metallographic examinations. The result of etching depends on many factors, including: the chemical composition of the etched material, the structure forming in the process, segregations in the material, both in the chemical composition and in the phases, and etching parameters (reagent type, reagent concentration, etching method, etching time). Based on the literature [16,17] and the authors' own experience, 6 reagents for chemical and electrochemical etching were selected. Examples of Inconel 617 structures revealed in the etching process are shown in Table 3.

TABLE 3

Procedure for preparing metallographic sections of Inconel 617

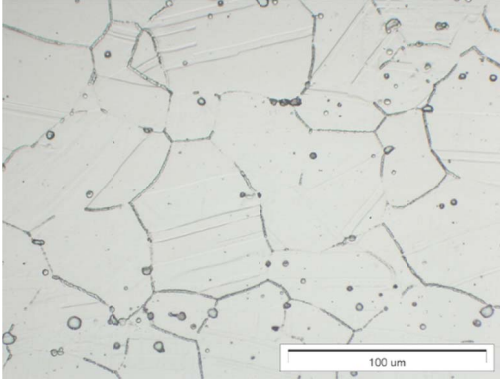
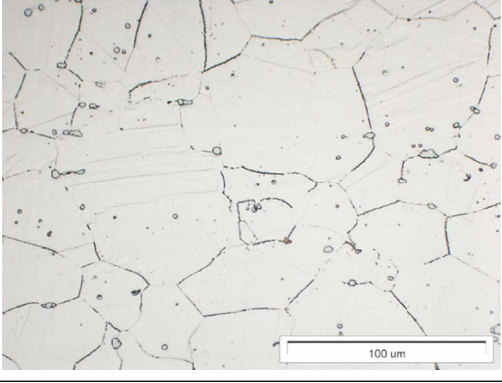
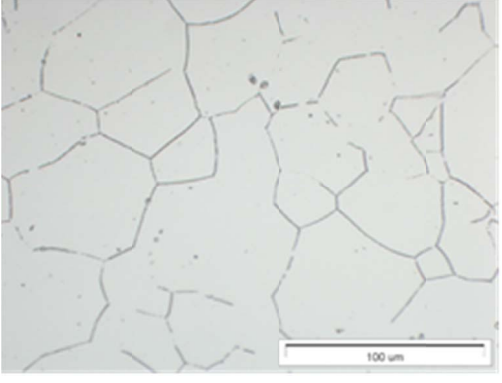
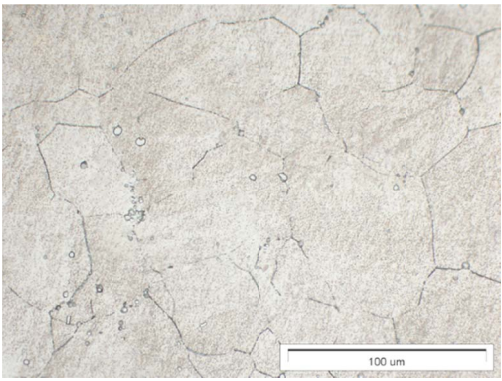
Stage	Material	Particle type	Rate	Time
1	P120 abrasive paper	SiC, water cooling	250 rpm, with the sample and the blade moving in the same direction	Until a flat surface is obtained
2	P220 abrasive paper	SiC, water cooling	250 rpm, with the sample and the blade moving in the same direction	Until a flat surface is obtained
3	P320 abrasive paper	SiC, water cooling	250 rpm, with the sample and the blade moving in the same direction	Until a flat surface is obtained
4	P500 abrasive paper	SiC, water cooling	250 rpm, with the sample and the blade moving in the same direction	Until a flat surface is obtained
5	P1200 abrasive paper	SiC, water cooling	250 rpm, with the sample and the blade moving in the same direction	Until a flat surface is obtained
6	Struers cloth	6 µm Metadi Supreme oil base – diamond suspension	150 rpm, with the sample and the blade moving in the opposite directions	2 minutes
7	Struers cloth	3 µm Metadi Supreme oil base – diamond suspension	150 rpm, with the sample and the blade moving in the opposite directions	3 minutes

Based on the etching tests conducted, it was determined that for the purposes of metallographic examinations, the best results were obtained for electrochemical etching in a 10% solution of oxalic acid at 6 V for 15 s (Table 4, item 1). Good results were

also obtained for Lucas' reagent (150 ml HCl, 100 ml $C_3H_6O_3$, 3 g $C_2H_2O_4$) at 6 V for 20 s (Table 4, item 2). In the other tests, the structure was not revealed in a manner guaranteeing correct metallographic examinations, either qualitative or quantitative.

TABLE 4

Structure of Inconel 617 revealed using various chemical reagents

	Reagent	Base material	Notes
1	10% aqueous solution of oxalic acid $C_2H_2O_4$; electrochemical etching 6 V for 15 s		Well-revealed grain boundaries, visible characteristic twins with phase precipitates along grain boundaries and within grains
2	150 ml HCl, 100 ml $C_3H_6O_3$, 3 g $C_2H_2O_4$ (Lucas' reagent); Electrochemical etching 6 V for 20 s		Well-revealed grain boundaries, visible characteristic twins with phase precipitates along grain boundaries and within grains
3	80 ml H_3PO_4 , 20 ml H_2O ; Chemical etching For 10 s		Revealed grain boundaries, visible phase precipitates along grain boundaries and within grains, no visible twins
4	15 ml HCl, 10 ml CH_3COOH , 10 ml HNO_3 ; Electrochemical etching 10 V for 15 s		Incorrectly revealed structure, difficulties in identifying precipitates and grain boundaries

3.4. Selection of the image acquisition method for metallographic examinations

Image acquisition in metallographic examinations should ensure legible, sharp images of the structure, enabling its qualitative description. The procedure for selecting an image acquisition method proposed below comprises two stages that ensure image repeatability and reproducibility. The first stage is the selection of a test stand and the second stage is the selection of an appropriate observation technique. The observations of the structure of Inconel 617 were carried out at test stands available at the Faculty of Materials Engineering and Metallurgy, i.e.

- a macroscopic examination stand equipped with a NIKON Coolpix 995 digital camera that enables observation at magnifications of up to 5 \times , both in the bright field and the dark field mode;
- a test stand equipped with an OLYMPUS SZX 9 stereoscopic microscope (SM) that enables observation at magnifications of up to 50 \times in the dark field;
- a microscope stand equipped with an OLYMPUS GX71 light microscope (LM) enabling observation at magnifications of up to 1000 \times . The use of a metallographic microscope for structural examinations makes it possible to use both bright field and dark field techniques, as well as special light microscopy techniques, i.e. polarized light and Nomarski interference contrast;
- a Hitachi S 3400N scanning electron microscope (SEM) and a Joel JCM 6000 microscope;
- a Hitachi S2300A scanning transmission electron microscope.

Examples of images of the macro- and microstructure and the substructure obtained at the test stands are shown in Table 5.

An analysis of the results obtained indicated that the test stand equipped with the digital camera was best suited for the visual assessment of the welded joint surface. This stage of the examination ensures the correct observation of the welded joint surface both on the face and the root sides (Table 5, items a, b). Examination of the face and the root should be carried out at magnifications not exceeding 5 \times in the bright field mode. The requirements of PN-EN ISO 5817 should be adopted as the criteria for assessing the quality of the welding.

The next stage of the metallographic examinations is an analysis of the welded joint macrostructure and an assessment of the shape of the weld fusion zone. Such examinations should be carried out at magnifications of up to 30 \times in the dark field mode under a SM (Table 5, items c-e). An important element of this stage is an assessment of the welding quality, and in particular of the quality level according to PN-EN ISO 5817.

Observations of the revealed structure of Inconel 617 under a LM indicate that metallographic examinations should be carried out in the bright field mode at magnifications not exceeding 500 \times . The images obtained confirm that the proposed procedure yields legible images ensuring the correct qualitative assessment of the structure of an Inconel 617 welded joint.

The metallographic examinations under a LM were complemented by observations at large magnifications LM under a SEM.

These were carried out using a Hitachi S 3400N microscope and a Joel JCM 6000 Neoscope microscope in the secondary electron (SE) and the back-scattered electron (BSE) imaging modes. Images recorded using the SE technique enable analysing structure topography, whereas BSE images reveal differences in the chemical composition.

The substructure of the material was analysed under a STEM microscope at magnifications above 10000 \times . The examinations were carried out on thin films prepared in accordance with a procedure developed at the Institute of Materials Engineering of the Silesian University of Technology. The preparation of the thin films of welded joints consisted in cutting the samples on an electrical discharge cutter into approx. 1 mm thick slices, which were subsequently ground on both sides until a thickness of 0.05 mm was reached. The electrochemical thinning was carried out using a Struers TenuPol-5 device at 45 V and 5 $^{\circ}$ C, in an electrolyte having the following composition: 70% CH₂OH, 20% glycerine, 10% HClO₄. Liquid nitrogen was used for cooling. At the final stage, the films were rinsed in water, methanol, and ethanol and dried.

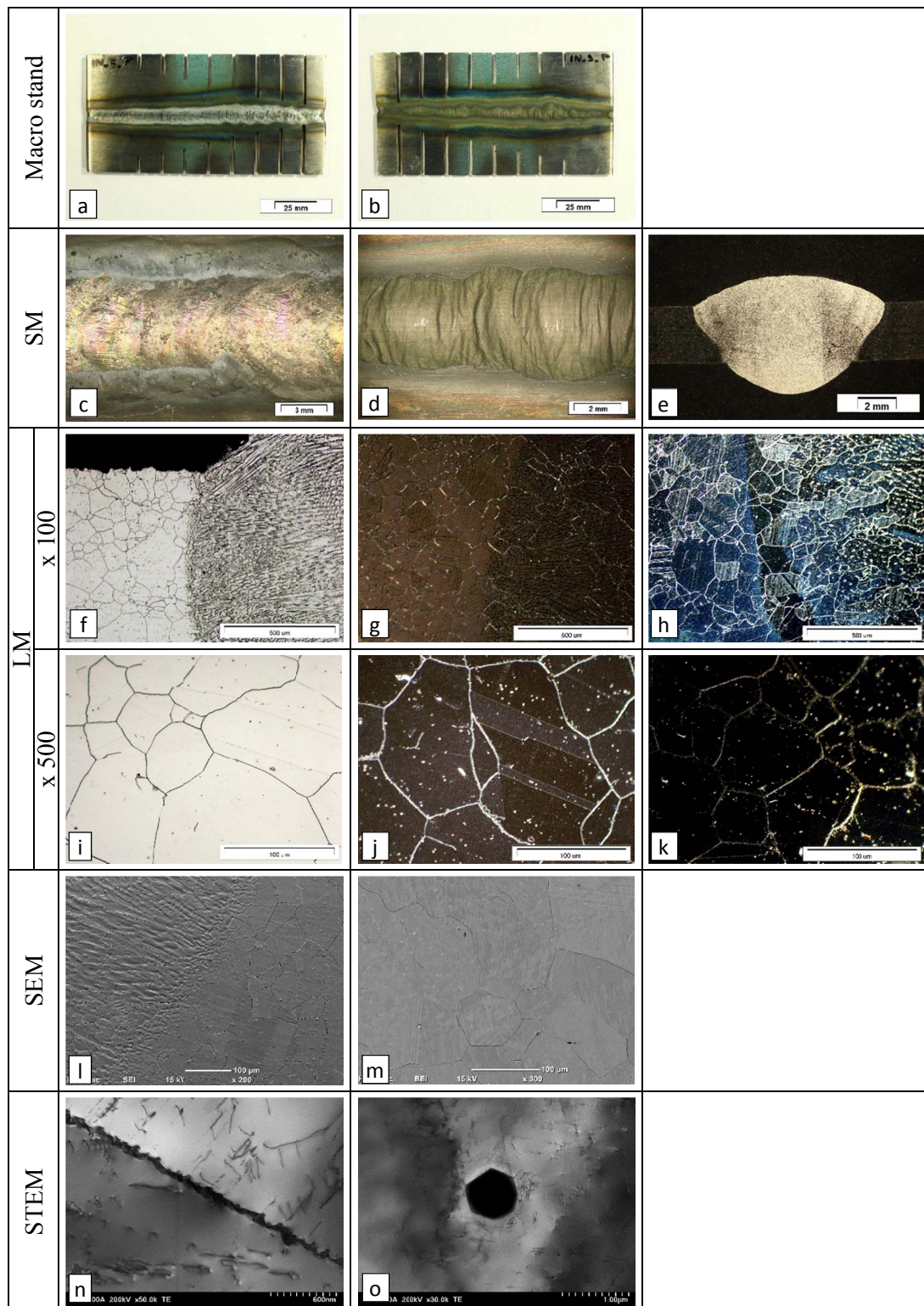
The substructure of the Inconel 617 welded joints was examined under a Hitachi 2300A STEM microscope using the thin film x-ray technique. The microscope is equipped with a Schottky field emission gun (FEG). The accelerating voltage during the examinations was 200 kV. A microanalysis of the chemical composition was performed using an energy-dispersive X-ray spectroscope (EDS) by Thermo Noran (System Seven), coupled with the Hitachi HD-2300A microscope.

3.5. Comprehensive procedure for assessing the structure of an Inconel 617 welded joint

The first stage of the procedure is the verification of the chemical composition. The best method, fast and non-destructive, for verifying the chemical composition is X-ray fluorescence (XRF). The method was used on a Niton XL2 device to verify the chemical composition of Inconel 617 against the manufacturer's specifications and ASME SB-168:2013.

The assessment of the macro- and microstructure of a welded joint should be carried out on metallographic sections cut out perpendicularly to the welding direction. Electrochemical etching in Lucas' reagent (Table 4, item 2) is recommended for revealing the structure of an Inconel 617 welded joint. The next stage is the assessment of the face and root quality. Visual examinations should be carried out in accordance with PN-EN ISO 17637. Subsequently, the macrostructure of the welded joint should be assessed. The examinations were carried out using a stereoscopic microscope (SM) in the dark field mode at magnifications of up to 50 \times . An analysis of the microstructure of the welded joint in all its zones, i.e. the base material, the heat affected zone, and the weld was performed at magnifications of up to 500 \times , using a light microscope (LM) in the bright field mode. These examinations should be complemented by observations under a scanning electron microscope (SEM) at magnifications

Results of the examination of the macro- and microstructure of Inconel 617 welded joints



of up to 5000 \times in the secondary electron (SE) mode and the back-scattered electron (BSE) mode. The substructure of the material was analysed at magnifications above 10000 \times using a scanning transmission electron microscope (STEM).

An EDS microanalysis of the chemical composition was performed in order to identify the chemical composition of the phases and precipitates present both in the base material and

in the welded joints. The examinations were carried out using a SEM equipped with an EDS chemical composition detector and the results obtained were complemented by an XRD analysis of the chemical composition and by electron diffraction on a STEM. This part of the procedure enables identifying the phases and components in the structure of the welded joint. The entire procedure is presented in the form of a diagram in Fig. 3.

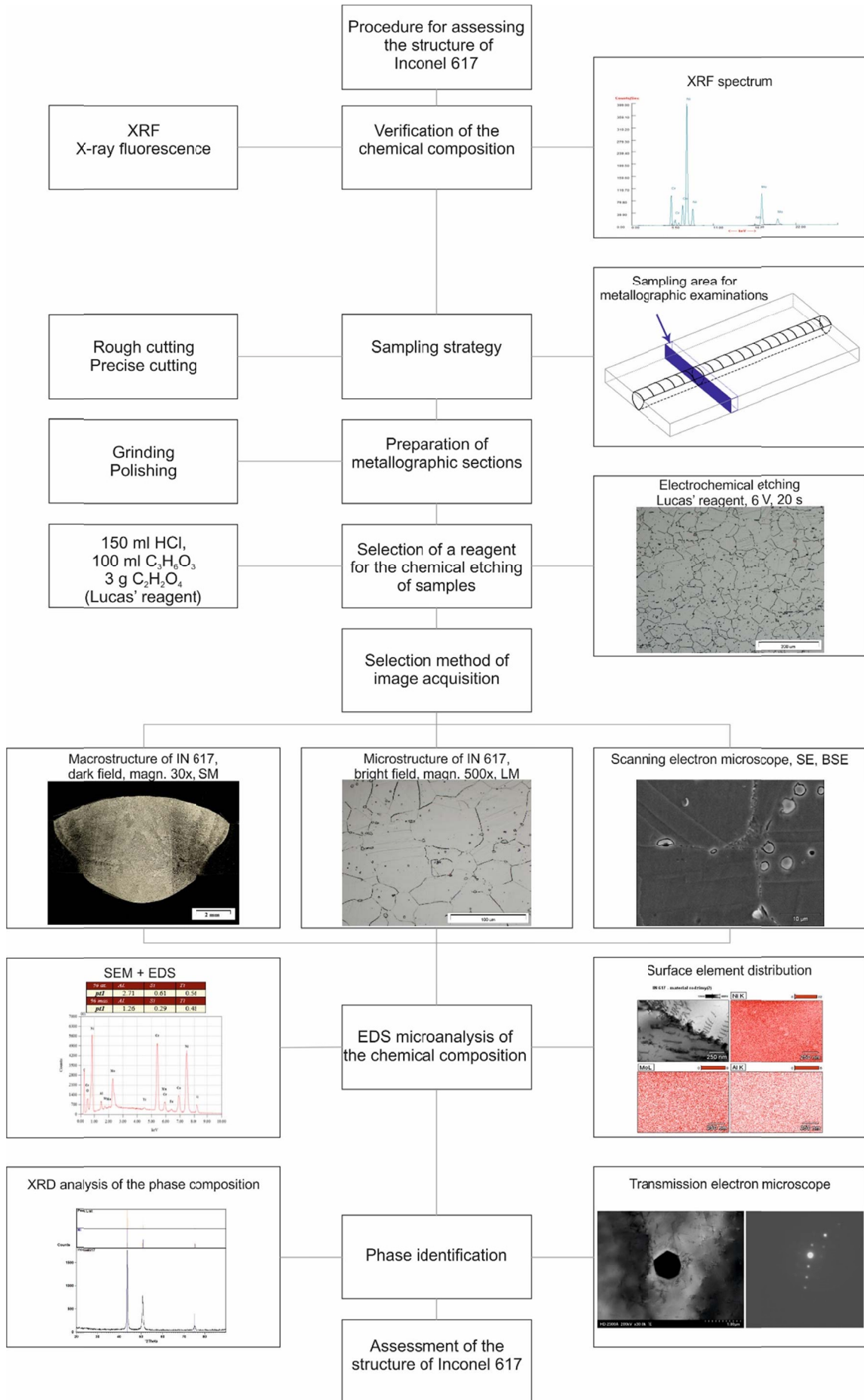


Fig. 3. Procedure for assessing the structure of Inconel 617

3.6. The structure of wrought Inconel 617

The proposed examination procedure enables not only the determination of the grain size based on standards, but also the identification of phases and substructural components that affect the properties of Inconel 617. Metallographic examinations carried out under a light microscope in accordance with the procedure described in section 2 confirmed the grain size assessment results obtained by the manufacturer and set out in appropriate specifications. A one-phase granular structure with visible twins and fine carbides was observed in the samples examined (Fig. 4).

According to the data provided in the specifications for the 1 mm thick plate (specification 27424, cast L40252), the average grain diameter is 44.9 μm (grain size number 6 according to ASTM E112), which was confirmed in the examinations (Fig. 4a,b). In the case of the 3 mm thick plate (specification 104727/0, cast 316343), the average grain diameter is 85-90 μm , which meets the requirements for grain size numbers 4.0 and 4.5

according to ASTM E112 (Fig. 4c, d). For the 5 mm thick plate (specification 95198/1, cast 331145), the average grain diameter is 74 μm , which corresponds to grain size number 4.5 according to ASTM E112 (Fig. 4e,f).

The structural examinations under a light microscope were complemented by observations under a SEM along with an EDS microanalysis of the chemical composition. The results of the structural examinations are presented in Fig. 5, whereas Fig. 6 and Fig. 7. show examples of results of the microanalysis of the chemical composition.

The results of phase identification in the structure of the plates, performed using the XRD method, confirmed the literature data. The main phase constituting the alloy's matrix is the γ phase (nickel solid solution) (Fig. 8).

The examinations under a STEM, in particular the electron diffraction and the microanalysis of the chemical composition, indicated that the γ light phase matrix (Fig. 9) also contained M_{23}C_6 carbides (Fig. 10-11).

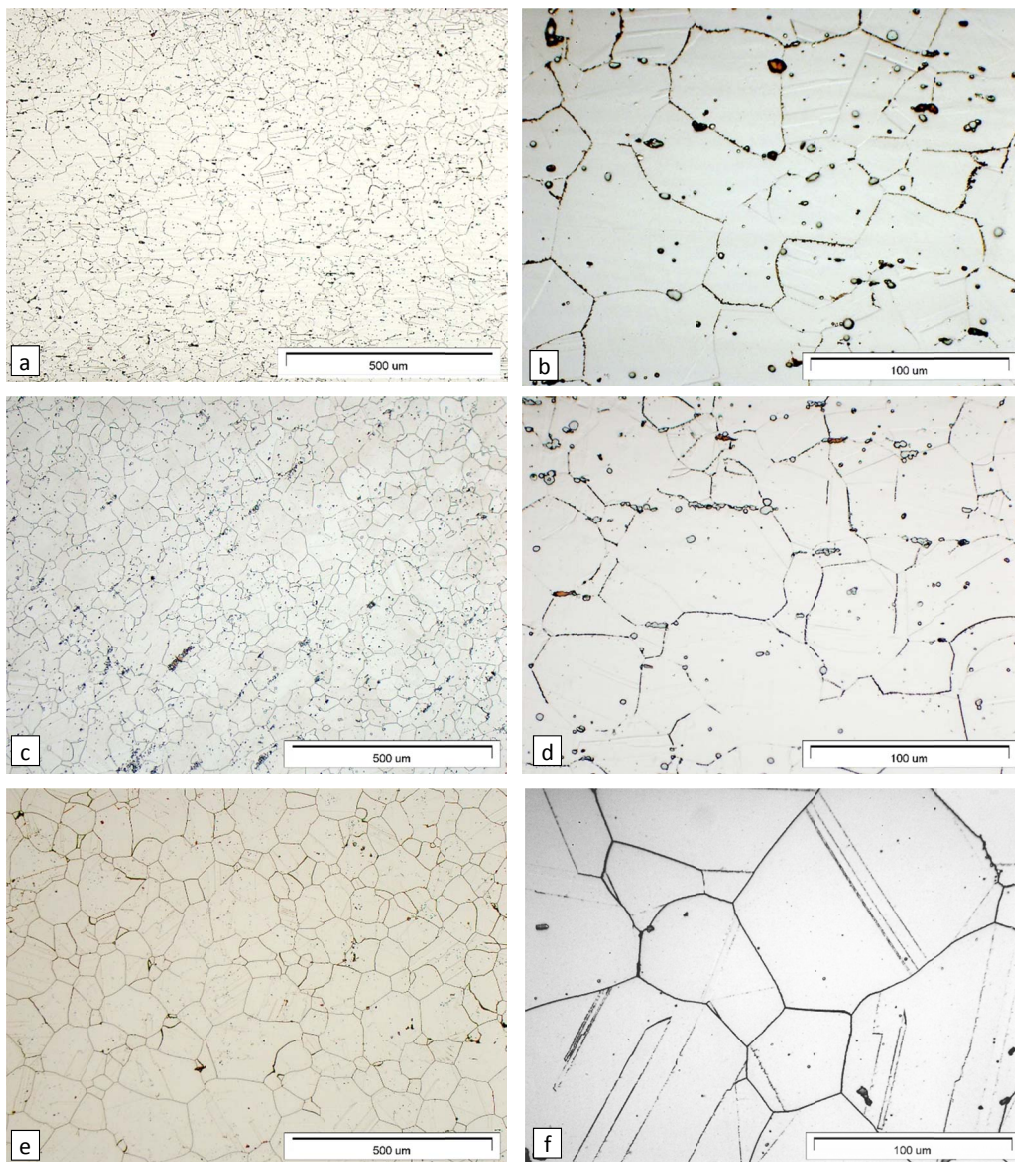


Fig. 4. Microstructures of Inconel 617, LM: a) 1 mm thick plate, magnification: 100 \times , b) 1 mm thick plate, magnification: 500 \times , c) 3 mm thick plate, magnification: 100 \times , d) 3 mm thick plate, magnification: 500 \times , e) 5 mm thick plate, magnification: 100 \times , f) 5 mm thick plate, magnification: 500 \times

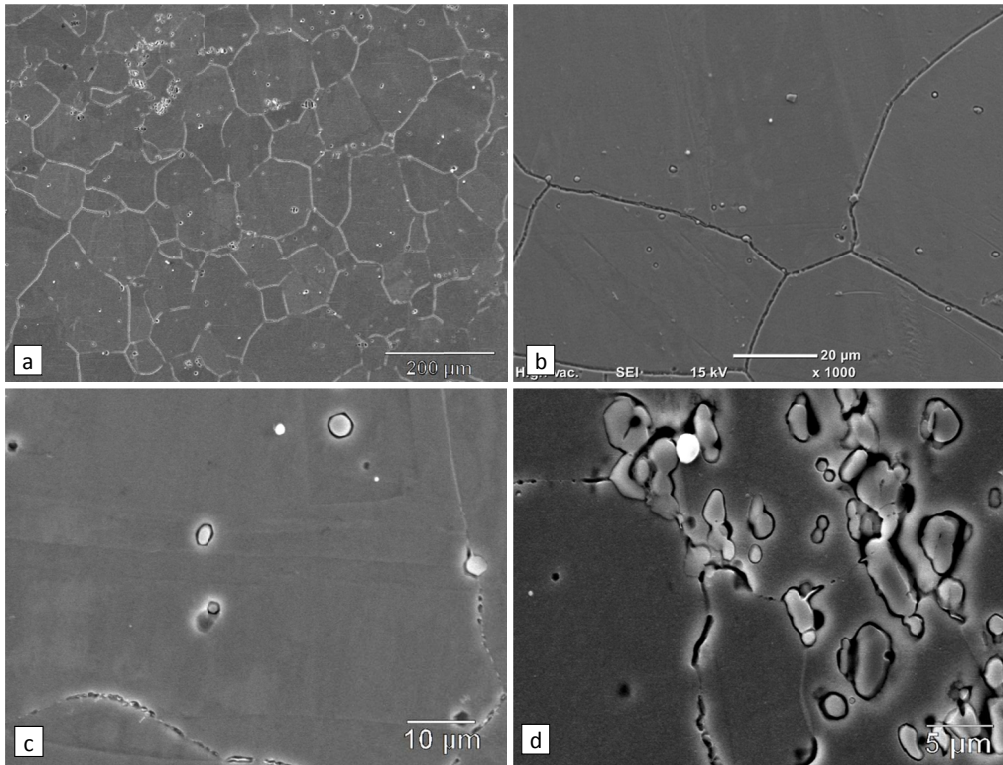
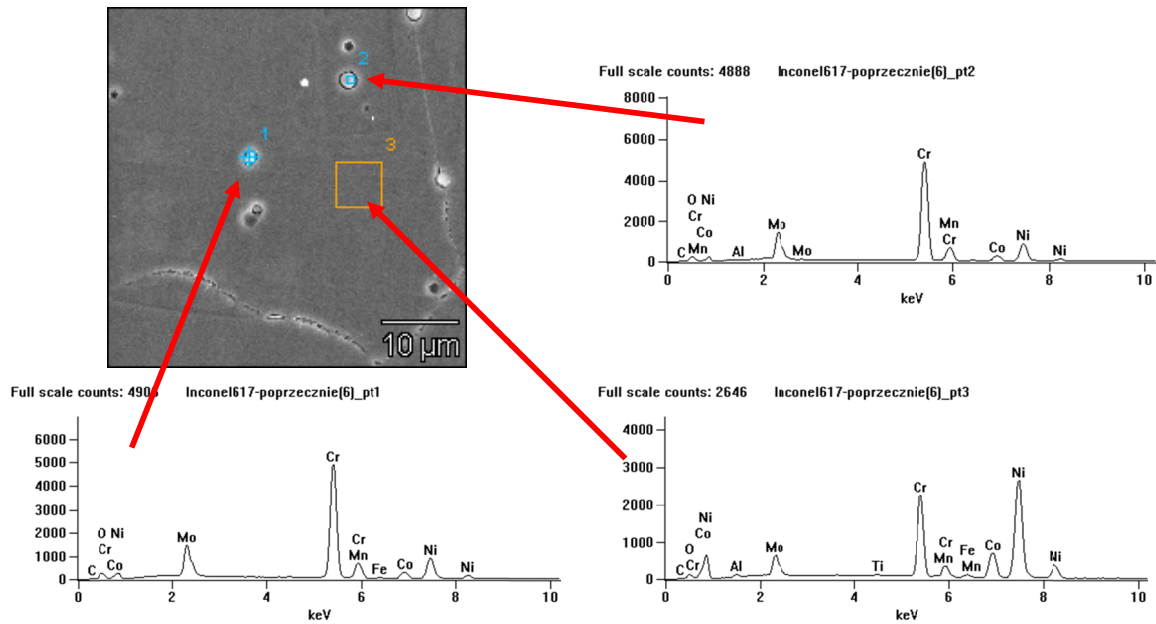


Fig. 5. Microstructure of Inconel 617, SEM: a) polygonal grains of the γ phase, magnification: 200 \times , SE, b) phase precipitates inside grains and along γ phase boundaries, magnification 1000 \times , SE, c) globular phase precipitates inside a grain and plate precipitates along the boundary, magnification: 5000 \times , SE, d) compound carbide precipitates, magnification: 10000 \times , BSE



% at.	Al	Ti	Cr	Mn	Fe	Co	Ni	Mo
pt1	-	-	64.0	0.1	0.4	5.2	18.6	11.7
pt2	0.6	-	63.4	0.3	0.3	5.5	18.3	11.6
pt3	2.3	0.4	25.7	0.1	0.8	11.4	53.9	5.3
% mas.	Al	Ti	Cr	Mn	Fe	Co	Ni	Mo
pt1	-	-	56.6	0.1	0.4	5.2	18.6	19.1
pt2	0.3	-	56.2	0.3	0.3	5.5	18.3	19.1
pt3	1.1	0.4	23.0	0.1	0.8	11.6	54.4	8.7

Fig. 6. EDS microanalysis of the chemical composition of Inconel 617, SEM

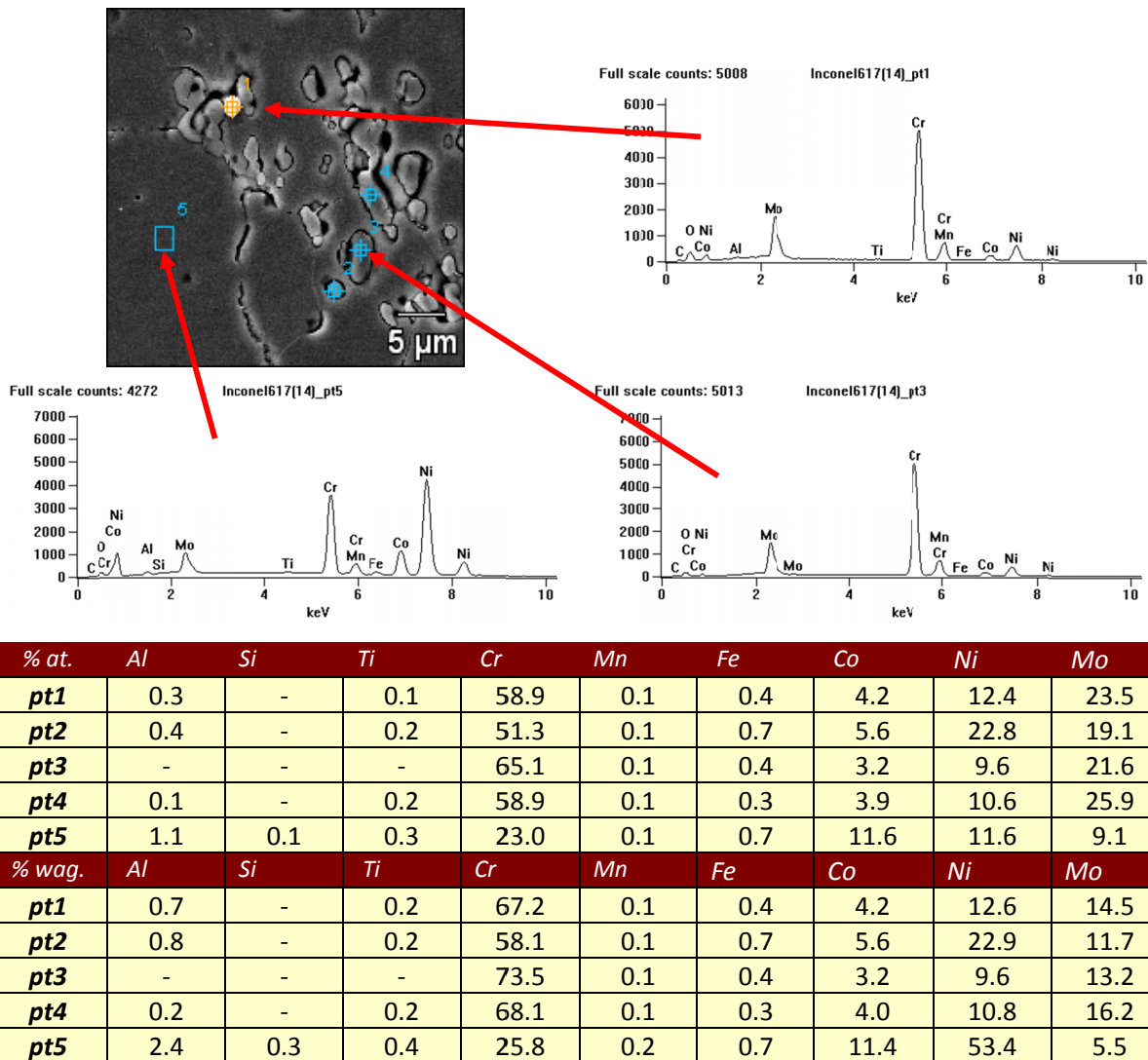


Fig. 7. EDS microanalysis of the chemical composition of Inconel 617, SEM

Based on the metallographic examinations, the EDS microanalysis of the chemical composition, the XRD phase analysis, and the identification of the phases revealed in the

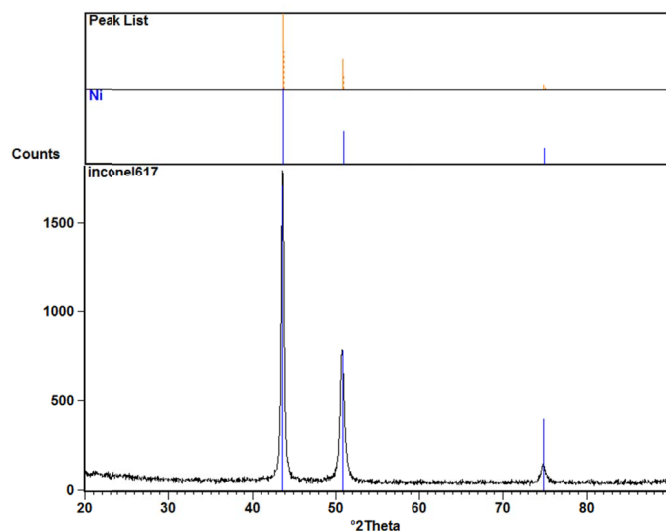


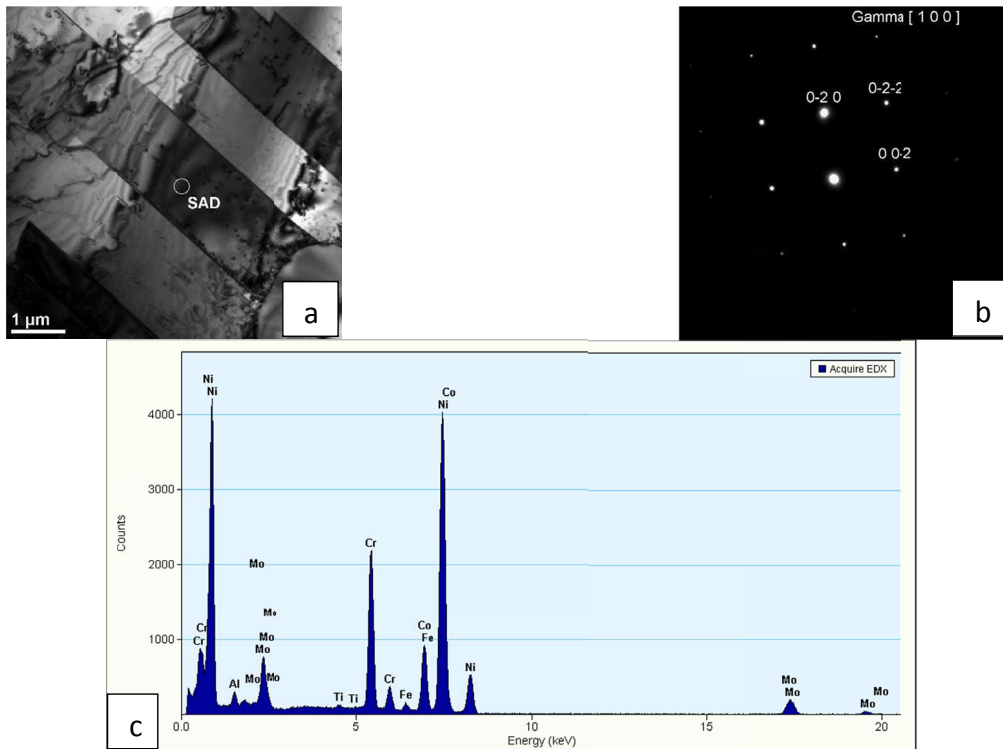
Fig. 8. Results of the XRD phase analysis of Inconel 617 plates

structure by means of electron diffraction, it was determined that the rolled Inconel 617 plates were built of polygonal γ phase grains with sparse plate precipitates of $M_{23}C_6$ carbides along grain boundaries and globular carbides inside grains. Sparse γ/γ' eutectic mixture areas and titanium nitrides were also identified in the structure.

4. Summary

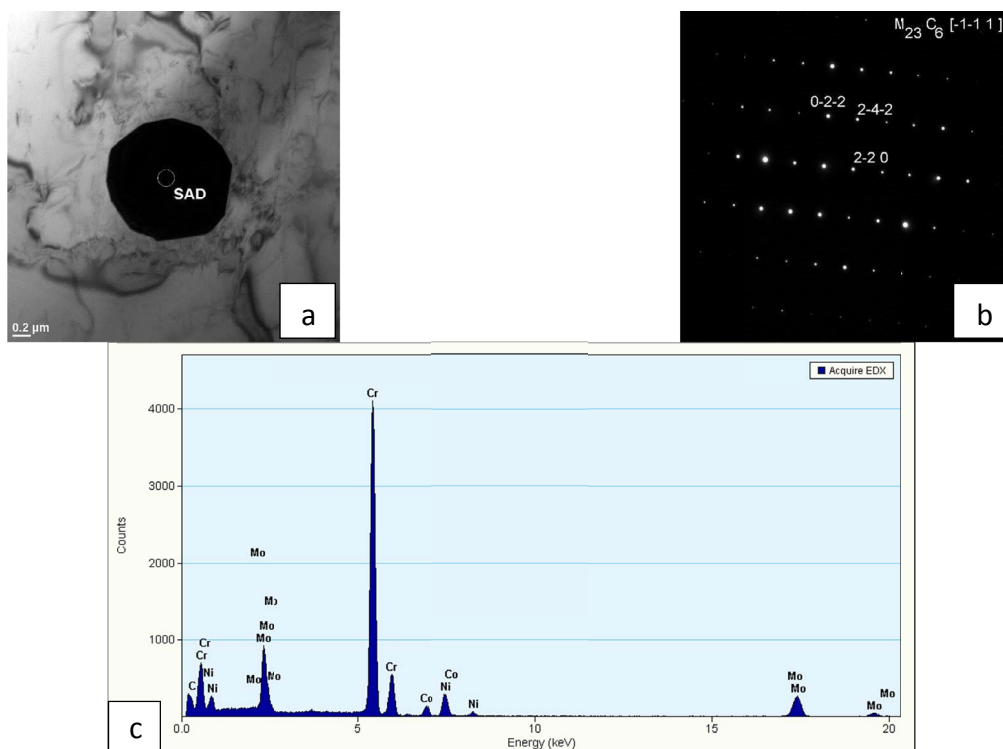
The proposed methodology for assessing the structure of Inconel 617 comprises the selection of a sampling area (Fig. 2), the manner of preparing metallographic sections (Table 2-3), the selection of a reagent for revealing the structure (Table 4), and the selection of an image acquisition method for metallographic examinations (Table 5). On this basis, a comprehensive procedure for assessing the structure of welded joints of Inconel 617 was developed, one that enables obtaining legible and reproducible results (Fig. 3).

Metallographic examinations carried out on a LM in accordance with the procedure illustrated in Fig. 3 confirmed that



% Mas.	Al	Ti	Cr	Fe	Co	Ni	Mo
	0.81	0.43	21.19	1.03	11.11	54.44	10.99

Fig. 9. Results of the electron diffraction of the Inconel 617 matrix: a) the structure of twins, with a marking indicating the analysis point, b) electron diffraction of the γ phase, c) results of the EDS microanalysis of the chemical composition of the analysed area



C	Cr	Co	Ni	Mo
6.58	62.88	2.56	5.34	22.64

Fig. 10. Results of the electron diffraction of the precipitates in Inconel 617: a) globular precipitate in a grain, b) electron diffraction of the $M_{23}C_6$ carbide, c) results of the EDS microanalysis of the chemical composition of the precipitate

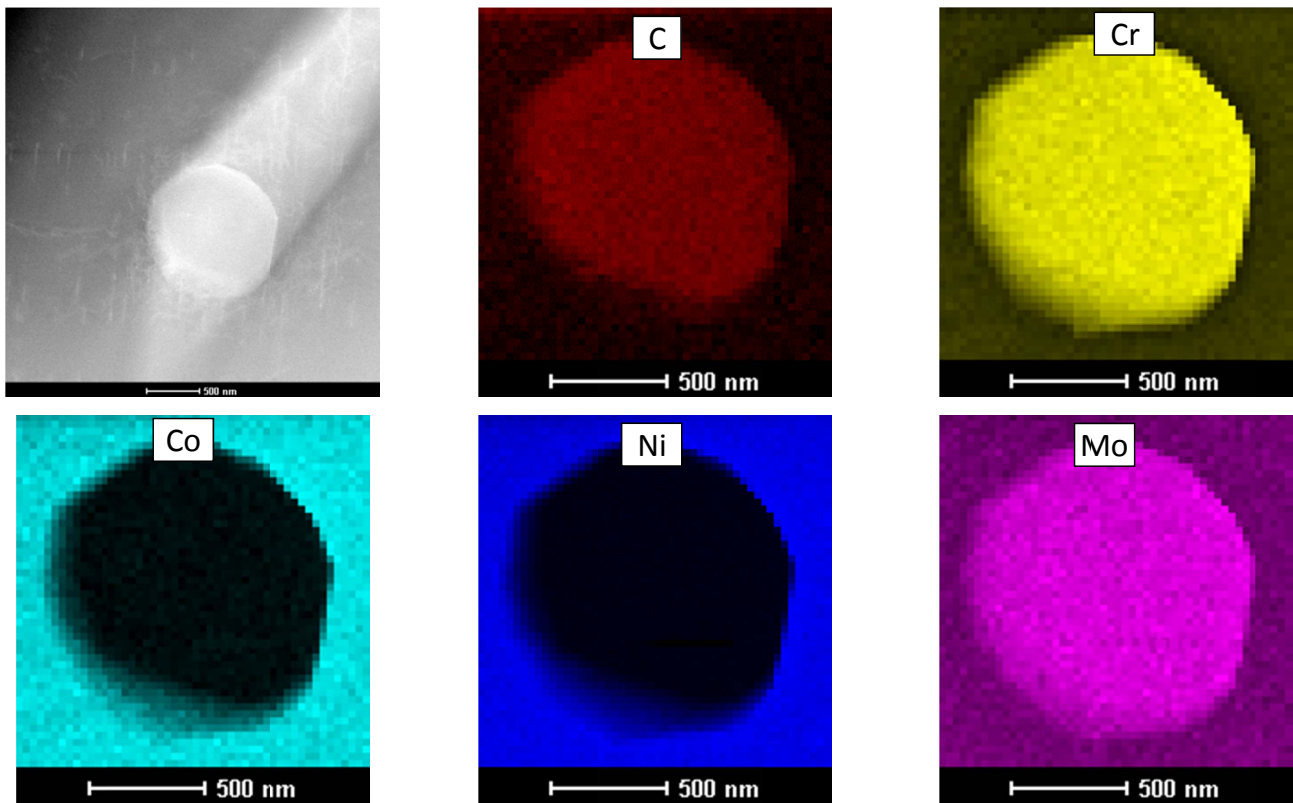


Fig. 11. Surface element distribution in chromium carbide $M_{23}C_6$

the Inconel 617 alloy was characterised by a one-phase granular structure. Moreover, numerous twins within grains and fine carbides were identified, which corresponds with the literature data [18-25] (Fig. 4). The results of the structural examinations under a LM were confirmed by observations under a SEM (Fig. 5). The EDS microanalysis of the chemical composition indicated that the precipitates in Inconel 617 mainly consisted of chromium, molybdenum, and carbon (Fig. 6-7), which may indicate $M_{23}C_6$ carbides. The XRD phase identification indicated that the main phase in Inconel 617 was the solid-solution-strengthened γ phase (Fig. 8), which is confirmed by the literature [26,27]. The electron diffraction on a SEM confirmed the presence of twins (Fig. 9) and $M_{23}C_6$ carbides (Fig. 10), made up of chromium and molybdenum (Fig. 11). According to the literature [1,2,27-30], secondary $(Mo, Cr)_{23}C_6$ carbides enhance the mechanical properties of Inconel 617, and especially its creep resistance, by inhibiting slipping along grain boundaries. They are mainly located along grain boundaries, in the form of globular precipitates, and they determine the high-temperature creep resistance (microstructural stability at high temperatures) of Inconel 617.

The proposed procedure, requiring reasonable effort and time, provides a legible, repeatable, and reproducible description of the structure of Inconel 617.

REFERENCES

- [1] H. Semba, T. Hamaguchi, M. Yoshizawa, H. Okada, A. Ishikawa, Development of Boiler Tubes and Pipes for Advanced USC Power Plants, in: Nippon Steel & Sumitomo Metal Technical Report, 71-77 (2015).
- [2] J.K. Wessel, Nickel and Nickel Alloy, The Handbook of Advanced Materials Enabling New Designs, John Wiley & Sons, New Jersey (2004).
- [3] S.J. Patel, J.J. deBarbadillo, B.A. Baker, R.D. Gollihue, Nickel Base Superalloys for Next Generation Coal Fired AUSC Power Plants, *Procedia Engineering* **55**, 246-252 (2013).
- [4] R. Viswanathan, J.F. Henry, J. Tanzosh, G. Stanko, J. Shingledecker, B. Vitalis, R. Purgert, U.S. program on materials technology for ultra-supercritical coal power plants, *Journal of Materials Engineering and Performance* **14**, 281-292 (2005).
- [5] J.R. Davis, Heat-Resistant Materials, ASM International, Printed in the United States of America, (1997).
- [6] S.F. Di Martino, R.G. Faulkner, S.C. Hogg, S. Vujic, O. Tassa, Characterisation of microstructure and creep properties of alloy 617 for high-temperature applications, *Materials Science and Engineering A* **619**, 77-86 (2014).
- [7] VDM Metals GmbH, Alloy 617 – Nicrofer 5520 Co, Material Data Sheet No. 4019. https://www.vdmmetals.com/fileadmin/user_upload/Downloads/Data_Sheets/Data_Sheet_VDM_Alloy_617.pdf, accessed 20 July 2019
- [8] M. Grudzień, L. Tuz, K. Pańcikiewicz, A. Zielińska-Lipiec, Microstructure and Properties of a Repair Weld in a Nickel Based Superalloy Gas Turbine Component, *Advances in Materials Science* **17**, 55-63 (2017).
- [9] S.P. Sridhar, S.A. Kumar, P. Sathiyaa, A study on the effect of different activating flux on A-TIG welding process of Incoloy 800H, *Advances in Materials Science* **16**, 26-37 (2016).

- [10] T. Chu, H. Xu, Z. Li, F. Lu, Investigation of intrinsic correlation between microstructure evolution and mechanical properties for nickel-based weld metal, *Materials & Design* **165**, 107595 (2019).
- [11] K. Mageshkumar, N. Arivazhagan, P. Kuppan, Studies on the effect of filler wires on micro level segregation of alloying elements in the alloy 617 weld fusion zone, *Materials Research Express* **11**, 116579 (2019).
- [12] C. Soares, *Gas Turbines: A handbook of air, land and sea applications*, Elsevier Science (2014).
- [13] J.R. Davis, *Nickel, Cobalt, and Their Alloys*, ASM International, (2000).
- [14] *Buehler's Guide to Materials Preparation*, Buehler (2005).
- [15] L. Bjerregaard, K. Geels, B. Ottesen, M. Ruckert, *Metallog Guide*, Suers A/S (2000).
- [16] Y. Guo, B. Wang, S. Hou, Aging Precipitation Behavior and Mechanical Properties of Inconel 617 Superalloy, *Acta Metallurgica Sinica* **26**, 307-312 (2013).
- [17] E. Gariboldi, M. Cabibbo, S. Spigarelli, D. Ripamonti, Investigation on precipitation phenomena of Ni-22Cr-12Co-9Mo alloy aged and crept at high temperature, *International Journal of Pressure Vessels and Piping* **85**, 63-71 (2008).
- [18] H.K.D.H. Bhadeshia, *Nickel Based Superalloy*, University of Cambridge. <http://www.phase-trans.msm.cam.ac.uk/2003/Superalloys/superalloys.html>, accessed 20 July 2019.
- [19] W. Liu, F. Liu, R. Yang, X. Tang, H. Cui, Gleeble simulation of the HAZ in Inconel 617 welding, *Journal of Materials Processing Technology* **225**, 221-228 (2015).
- [20] M. Akbari-Garakani, M. Mehdizadeh, Effect of long-term service exposure on microstructure and mechanical properties of Alloy 617, *Materials & Design* **32**, 2695-2700 (2011).
- [21] M. Cabibbo, E. Gariboldi, S. Spigarelli, D. Ripamonti, Creep behavior of INCOLOY alloy 617, *Journal of Materials Science*, **43**, 2912-2921 (2008).
- [22] X. Li, D. Kininmont, R. Le Pierres, S.J. Dewson, Alloy 617 for the High Temperature Diffusion-Bonded Compact Heat Exchangers, *Proceedings of ICAPP*, Anaheim, USA, June 8-12, 282-288 (2008).
- [23] M.S. Rahman, G. Priyadarshan, K.S. Raja, C. Nesbitt, M. Misra, Characterization of high temperature deformation behavior of Inconel 617, *Mechanism Mater* **4**, 261-270 (2009).
- [24] T.K. Yeh, H.P. Chang, M.Y. Wang, T. Yuan, J.J. Kai, Corrosion of Alloy 617 in high-temperature gas environments, *Nuclear Engineering and Design* **27**, 257-260 (2014).
- [25] F. Tahir, S. Dahire, Y. Liu, Image-based creep fatigue damage mechanism investigation of Alloy 617 at 950 °C, *Materials Science & Engineering A* **679**, 391-400 (2017).
- [26] D.C. Tung, J.C. Lippold, Weld solidification behaviour of Ni-base superalloys for use in advanced supercritical coal-fired power plants, in: *Superalloys 2012: 12th International Symposium on Superalloys*, The Minerals, Metals & Materials Society, 563-567 (2012).
- [27] L. Ma, Identifying and Understanding Environment-Induced Crack Propagation Behavior in Solid Strengthened Ni-Based Superalloys, Project No. 09-803, University of Nevada, 2012. https://neup.inl.gov/SiteAssets/Fijnal%20%20Reports/NEUP_Project_No_09-803_Final_Report.pdf, accessed 20 July 2019.
- [28] D. Tytko, P. Choi, J. Klower, A. Kostka, G. Inden, D. Raabe, Microstructural evolution of Ni-based superalloy (617B) at 700°C studied by electron microscopy and atom probe tomography, *Acta Materialia* **60**, 1731-1740 (2012).
- [29] A. Hernas, *Żarowytrzymałość stali i stopów*, Wydawnictwo Politechniki Śląskiej (2000).
- [30] L.E. Shoemaker, J.R. Crum, *Nickel – Chromium – Molybdenum Superalloys: The Solution to Corrosion Problems in Wet Limestone FGD Air Pollution Control Systems*, Special Metals Corporation, 3200 Riverside Drive Huntington, WV 25705, USA 2014.